Contents lists available at ScienceDirect

Agricultural and Forest Meteorology

journal homepage: www.elsevier.com/locate/agrformet

Flux variance similarity-based partitioning of evapotranspiration over a rainfed alfalfa field using high frequency eddy covariance data

Pradeep Wagle[a,*], Todd H. Skaggs[b], Prasanna H. Gowda[c], Brian K. Northup[a], James P.S. Neel[a]

[a] Grazinglands Research Laboratory, USDA, Agricultural Research Service, El Reno, OK 73036, USA
[b] U.S. Salinity Laboratory, USDA, Agricultural Research Service, Riverside, CA 92507, USA
[c] USDA, Agricultural Research Service, Southeast Area, Stoneville, MS 38776, USA

ARTICLE INFO

Keywords:
Fluxpart
Evaporation
Transpiration
Water use efficiency

ABSTRACT

Although the eddy covariance (EC) technique provides direct and continuous measurements of evapotranspiration (ET), separate measurement of evaporation (E) and transpiration (T) at the ecosystem level is not possible. For partitioning ET into E and T, high frequency (10 Hz) time series EC observations collected from Apr 2016 to May 2018 over a rainfed alfalfa (*Medicago sativa* L.) field in central Oklahoma, USA were analyzed using the open source software Fluxpart. Fluxpart partitions ET by examining the correlation (R_{qc}) between water vapor (q) and carbon dioxide (c) fluxes as prescribed by the Flux Variance Similarity (FVS) partitioning method. Patterns of R_{qc} and partitioned E and T were consistent with expected trends associated with vegetation dynamics and short-term transient features (i.e., hay harvesting and rainfall events). The R_{qc} grew stronger with increasing alfalfa leaf area and exhibited a strong anti-correlation (R_{qc} close to -1) during peak growth when T and photosynthesis (P) were dominant and co-regulated by the leaf stomata. Consequently, a strong linear relationship (R^2 = 0.96) was found between monthly midday average values of R_{qc} and monthly average Moderate Resolution Imaging Spectroradiometer (MODIS)-derived leaf area index (LAI_{MOD}). Decorrelation of q and c or dominance of non-photosynthetic (e.g., E and respiration, R) fluxes resulted in less negative or positive R_{qc} values during winter, hay harvest, rainy, and nighttime periods. Growing season (Apr-Oct) average T:ET was approximately 0.82 and 0.77 in 2016 and 2017, respectively. Diurnal cycles and temporal variations of leaf-level water use efficiency (WUE, an input of the FVS method) estimates were consistent with the seasonal dynamics of ecosystem WUE, computed from EC-derived gross primary production (GPP) and EC-measured ET. These results validate the performance of the FVS ET partitioning method using high frequency EC data.

1. Introduction

Quantifying evapotranspiration (ET) is fundamental for a better understanding of agro-ecosystems and allocation of scare water resources since ET is a key component of the hydrological cycle that accounts for up to 95% of the water budget in dry agriculture (Wilcox et al., 2003). In recent years, the eddy covariance (EC) method has been widely used to measure high frequency (i.e., 10 Hz or higher) observations of the exchange of carbon dioxide (c) and water vapor (q) fluxes simultaneously at the landscape level (Baldocchi, 2014). Although EC can provide direct and continuous measurements of ET, it cannot provide separate measurements of the two components of ET: evaporation (E, nonproductive water use) and transpiration (T, productive water use enhancing plant productivity). It is difficult to determine individual components E and T at the landscape level through measurement (Burt et al., 2005; Wang et al., 2016; Williams et al., 2004). The partitioning of ET has important implications not only for the water budget but also for a mechanistic understanding of biological and climatic controls of E and T (Ferretti et al., 2003; Wang et al., 2015) since these two components are controlled by different processes and respond differently to climatic factors (Kool et al., 2014). Thus, the partitioning of ET into E and T is crucial to minimize the nonproductive loss of water and to improve water management practices and productivity of agroecosystems. Partitioning can also offer greater insights into the function of agroecosystems by reducing uncertainties in the interpretation of the coupling between water and carbon/nutrient cycles (Austin et al., 2004). In addition, partitioning is useful for improving the performance of land surface models as they are poorly constrained due to a lack of observations of the diurnal and seasonal variations of ET partitioning (Lawrence et al., 2007). However, the

* Corresponding author.
E-mail address: pradeep.wagle@usda.gov (P. Wagle).

https://doi.org/10.1016/j.agrformet.2020.107907
Received 2 October 2019; Received in revised form 10 January 2020; Accepted 14 January 2020
Available online 28 January 2020
0168-1923/ Published by Elsevier B.V.

partitioning of ET into E and T is still theoretically and technically challenging.

The exchanges of q and c are tightly coupled ecosystem processes (Morales et al., 2005). Direct measurements of carbon gain and water loss by EC allow us to quantify water use efficiency (WUE) at the ecosystem level (Law et al., 2002; Wagle and Kakani, 2014a), which reflects the trade-off between water loss and carbon uptake in carbon assimilation process. However, direct measurement of WUE solely based on T (i.e., productive water use) is not possible by EC due to the lack of separate measurements of E and T.

There are various methods to partition ET into E and T (Kool et al., 2014; Sutanto et al., 2014). The ET partitioning methods range from the conventional technique of integrating hydrometric T measurements (i.e., sap flow) with E measurements (i.e., weighing lysimeter) (Herbst et al., 1996; Kelliher et al., 1992) to more recent techniques based on analyzing the isotopic composition of liquid water and water vapor (Sutanto et al., 2012; Yepez et al., 2005), and to modeling approaches such as global land surface models (Miralles et al., 2011), the HYDRUS-1D model (Simunek et al., 2005), and two source surface energy balance (SEB) models (Norman et al., 1995). However, all these methods have limitations due to experimental difficulties or uncertainties or issues of spatial and temporal coverages in the measurement of E and T.

The Flux Variance Similarity (FVS) ET partitioning method had been proposed nearly a decade ago to partition E and T using high frequency EC data (Scanlon and Kustas, 2010, 2012; Scanlon and Sahu, 2008). A few recent studies have employed the FVS partitioning method to compare with other partitioning approaches (Klosterhalfen et al., 2019a; Palatella et al., 2014; Peddinti and Kambhammettu, 2019; Perez-Priego et al., 2018; Sulman et al., 2016). Some studies evaluated the performance of the FVS partitioning method for different land cover types: a suburban grass field (Wang et al., 2016), citrus orchards (Peddinti and Kambhammettu, 2019), a Mediterranean cropping system (Rana et al., 2018), and across gradients of woody plant cover (Wang et al., 2010). A few studies have performed sensitivity analysis of partitioning results using various estimates of leaf-level WUE (Klosterhalfen et al., 2019b; Sulman et al., 2016). Although EC measurements are available across the world through several EC networks (e.g., FLUXNET, AmeriFlux, EUROFLUX, AsiaFlux, ChinaFlux), wider testing and validation of the FVS partitioning method is still scarce, most likely due to the computational complexity of analyzing high frequency EC data. To permit wider practical applicability, the open source software Fluxpart has recently been developed to implement the FVS partitioning method (Skaggs et al., 2018). Details on the FVS flux partitioning method are available in the above-mentioned studies.

This study employed Fluxpart to partition and quantify the dynamics of E and T by examining q-c correlations (R_{qc}), and to characterize the biological and physical processes controlling the temporal dynamics of E, T, and R_{qc} over an alfalfa field (*Medicago sativa* L.). The alfalfa field was harvested periodically (4–5 times per year) and the study period consisted of two contrasting years: dry year 2016 (~32% less rainfall compared to the 30-year, 1981–2010, mean of 925 mm) and wet year 2017 (~20% more rainfall compared to the 30-year mean). Thus, this study can serve as a suitable case study for testing FVS ET partitioning method using the q-c correlation from high frequency (10 Hz) EC data.

2. Materials and methods

2.1. EC data description and processing

Using an EC system, high frequency (10 Hz) observations of exchange of c and q between a 48 ha Alfalfa field (cv. Cimarron 400 planted in Fall 2012) and the atmosphere were recorded from Apr 2016 to May 2018 at the United States Department of Agriculture-Agricultural Research Service, Grazinglands Research Laboratory, El Reno, Oklahoma, USA. The EC system, mounted at a height of 2.5 m above the ground surface, comprised of an open path infrared gas analyzer (LI-7500 RS, LI-COR Inc., NE, USA) and a 3-D CSAT3 sonic anemometer (Campbell Scientific Inc., UT, USA). The fetch length for the EC system was >200 m in each direction. Additional supporting meteorological measurements at the site included air temperature (T_a), relative humidity, photosynthetic photon flux density (PPFD), and net radiation (R_n). Near surface soil moisture (SM), soil temperature (T_s), and soil heat (G) fluxes were also collected. Rainfall data were collected from a nearby Oklahoma Mesonet (El Reno) station (http://mesonet.org/, accessed April 19, 2019). The alfalfa field was harvested four times in 2016 (cumulative forage yield of ~7.5 dry t ha^{-1}) and five times in 2017 (cumulative forage yield of ~10 dry t ha^{-1}) for hay.

Raw EC data were processed using the EddyPro software (version 6.2.0 - LI-COR Inc., Nebraska, USA) to compute 30-min ET values. Processed ET data were screened for bad quality flag 2, implausible values, and statistical outliers (beyond ± 3.5 standard deviation) based on a 14-day running window (Wagle et al., 2019a; Wagle and Kakani, 2014b). To retain pulses during certain times of the year (e.g., rain events), four or more consecutive reliable ET values beyond ± 3.5 standard deviation on a day were not considered outliers. Gaps in eddy fluxes and meteorological data were filled using the REddyProc package (https://www.bgc-jena.mpg.de/bgi/index.php/Services/REddyProcWebRPackage) from the Max Planck Institute for Biogeochemistry, Germany (Wutzler et al., 2018). Details on instrumentation and data processing for this site are explained in previous papers (Wagle et al., 2019a, 2019b).

2.2. Satellite remote sensing data

The 8-day composite values of the Moderate Resolution Imaging Spectroradiometer (MODIS)-derived leaf area index (LAI_{MOD}) for one pixel (~500 m × 500 m) containing the EC system were obtained from the Oak Ridge National Laboratory's Distributed Active Archive Center (ORNL DAAC, 2017). The LAI_{MOD} was binned into seven classes of increasing LAI as <0.5, 0.5–1, 1–1.5, 1.5–2, 2–2.5, 2.5–3, and >3 to examine the effect of LAI on q-c correlations.

2.3. Partitioning of ET into E and T using Fluxpart

To partition ET into E and T, the FVS flux partitioning method was performed on the 10 Hz frequency time series EC data from Apr 2016 to May 2018 using Fluxpart version 0.2.4 (Skaggs et al., 2018). Fluxpart applies basic QA/QC to high-frequency EC data and corrects high frequency data for external fluctuations associated with T_a and vapor density effects (Detto and Katul, 2007; Webb et al., 1980). A discrete wavelet decomposition is used in Fluxpart to progressively remove low frequency components from the high frequency data if partitioning results are not successful initially (Klosterhalfen et al., 2019b; Skaggs et al., 2018). For simplicity, a recent study applied a moving mean filter to the Reynolds decomposition of high-frequency time series (Scanlon et al., 2019). The FVS method requires leaf-level WUE as an input and assumes constant over a given data interval. In the absence of direct measurements of WUE, the default method used by Fluxpart to estimate WUE is:

$$WUE = 0.625\frac{c_a - c_i}{q_a - q_i}$$

where c_a and c_i are the ambient and intercellular carbon dioxide concentrations, and q_a and q_i are the ambient and intercellular water vapor concentrations, respectively. The ratio of molecular diffusivities for q and c is 0.625 (Massman, 1998). The ambient c and q concentrations were derived from EC tower measurements by extrapolating a logarithmic mean profile with stability corrections to the zero-plane displacement height (Scanlon and Kustas, 2010). The intercellular q

concentration equates to 100% relative humidity for a given leaf temperature where the leaf temperature is assumed to be equal to the above-canopy T_a (Skaggs et al., 2018). However, vapor pressure inside leaves may not remain saturated under all conditions (Cernusak et al., 2018). In Fluxpart, the intercellular c concentration can be a constant ppm value or c_i:c_a can be a function of the atmospheric vapor pressure deficit (VPD) (Katul et al., 2009; Morison and Gifford, 1983). If the parameter values are not provided as inputs then default parameter values are provided for C_3 and C_4 plants in all cases. We used the Fluxpart 0.2.4 default parameterization for C_3 plants which specifies that c_i:c_a is a constant value equal to 0.7. Cumulative values of partitioned fluxes were computed using interpolated values for the periods when the FVS partitioning method did not produce outputs. The source code of Fluxpart are accessible at https://github.com/usda-ars-ussl/fluxpart (accessed April 19, 2019).

2.4. Environmental impacts on temporal dynamics of R_{qc}

We examined the impacts on R_{qc} of four major environmental variables (PPFD, VPD, T_a, and SM) which can affect stomatal processes. Analyses were done using 30 min values during a selected peak growth period (Apr 15–28, 2017).

3. Results and discussion

3.1. Patterns of ET, E, and T

The 2017 growing season was wetter than the 2016 growing season (Fig. 1). The site received total rainfall of 501 mm and 930 mm during the 2016 and 2017 growing seasons (Apr-Oct), respectively. Thus, cumulative forage yield of alfalfa was also higher in 2017 (~10 dry t ha^{-1}) than in 2016 (~7.5 dry t ha^{-1}) (Wagle et al., 2019b). Total rain for Jan-Apr 2018 was only 101 mm (~0.6 times less than the 30-year mean of ~250 mm). As a result, ET values were higher during the 2017 growing season than during the drier 2016 growing season and spring 2018 (Fig. 1). As T is controlled by physiological control of leaf stomata, it is tightly coupled with plant tissue properties (Matheny et al., 2014; Sperry and Love, 2015). In addition, it responds to environmental drivers such as dry and wet conditions. In comparison, E is not directly linked to biological processes, but it responds to environmental drivers such as dry and wet conditions. Consequently, similar to ET, E and T values were also higher during the 2017 growing season than during the 2016 growing season and spring 2018 (Fig. 2).

There was >100 mm rain on Apr 29, 2017. Effects of rainfall and hay harvesting on surface energy fluxes (e.g., ET and NEE) were compared for rainy (Apr 29), pre-harvest (May 1), and post-harvest (May 4) days (Fig. 3a). The increased soil water availability after rainfall had a substantial effect on ET on May 4, 2017 even after hay harvesting. Comparison of ET between May 1 and 4 could not indicate that the field was harvested for hay before May 4. Rates of ET were only slightly higher on May 1 (pre-harvest) than May 4 (post-harvest), but the harvesting of hay was clearly reflected by NEE. The alfalfa field was a carbon source (positive NEE) for the entire day on May 4, but a carbon sink (negative NEE) on May 1. The magnitudes of both ET and NEE were smaller on the rainy day (Apr 29). When rates of NEE and ET were compared between pre-harvest and post-harvest dates during a dry period (Fig. 3b), the magnitudes of ET and NEE were substantially higher on Jun 6, 2017 (pre-harvest) than on Jun 8, 2017 (post-harvest). A large difference in NEE but similar ET between pre-harvest (May 1) and post-harvest (May 4) periods indicates the dominance of the E component after a big rainfall event. This result was further supported by the partitioning of E and T on those days (Fig. 4). The magnitude of T at pre-harvest (~0.25 mm 30 min^{-1}) was almost double than that at post-harvest (~0.12 mm 30 min^{-1}).

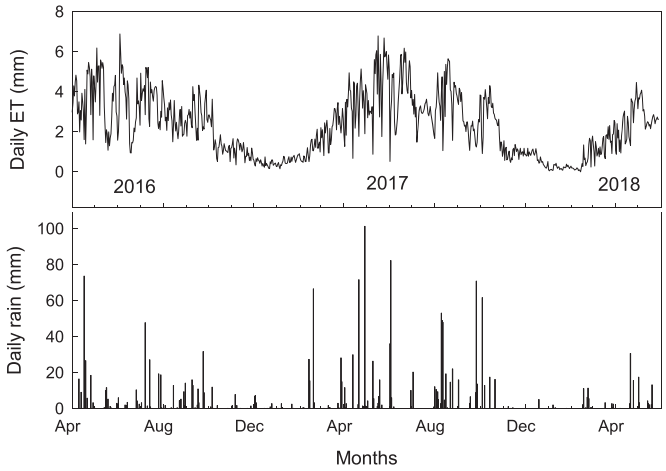

Fig. 1. Dynamics of daily evapotranspiration (ET) and rain for the study period.

3.2. Proportions of E and T to ET

The proportions of T or E to ET at around midday (average ratios from 11:00 am to 2:00 pm local time) for the 2016 and 2017 growing seasons are shown in Fig. 5. During the growing season, T dominated with T:ET approaching 1. An abrupt change in T:ET occurred immediately after rains or harvesting of hay with E increasing at the expense of T. The E:ET ratio was ~0.2 or less if hay harvesting and rainy periods were excluded. The fraction of E reached ~50% of total ET during hay harvesting or rainy periods.

Diurnal patterns of E and T were determined during peak growth (May 25–28) with no rainy days in 2017 (Fig. 6). The T peaked (~0.3 mm 30 min^{-1}) at ~2:00 pm, around the time radiation peaked, but E peaked (~0.15 mm 30 min^{-1}) before noon. If diurnal mean values were summed then daily ET was 6.16 mm, daily T was 4.55 mm, and daily E was 1.61 mm. When cumulative ET, T, and E were computed for this period (May 25–28, 2017), using interpolated partitioned fluxes, they were 24.3, 18.5, and 5.8 mm, respectively. The results indicated that nearly 25% of total ET was lost as E during peak growth. When T:ET was compared for selected pre-harvest (May 1–15), post-harvest/regrowth (May 19–25, 2016), and winter (Dec 16–30, 2016) periods, T accounted for 81%, 76%, and 70%, respectively, of the total ET (data not shown). The results illustrated the differences in diurnal cycles and temporal variations of ET partitioning. Such understanding of the diurnal cycles and temporal variations of ET partitioning can help to improve the performance of land surface models for water budgets, weather prediction, and climate studies (Betts et al., 1996; Lawrence et al., 2007).

Fig. 7 shows that the T:ET ratio was nearly 0.80 or higher in each month of the 2016 growing season (Apr-Oct). The T:ET ratio reached 0.83–0.85 during relatively hotter and drier Jun and Jul 2016. Similarly, T:ET was ~0.70 in May, Aug, and Oct 2017, while it reached 0.85–0.86 during relatively hotter and drier Jun and Jul 2017. Summers are generally warmer and drier in the region with a bimodal rainfall pattern (rain during spring and fall, with hot and dry summers). Even in a wet year 2017, near-surface (~5 cm depth) monthly average SM was approximately 0.12 and 0.08 m^3 m^{-3} in Jun and Jul, respectively, as compared to the monthly average SM of ~0.20 m^3 m^{-3} in both May and Aug. However, deep rooted perennial alfalfa stands can extract SM from deeper depths during dry summer periods. Reduced E from relatively drier top soil in summer can be attributed to relatively higher T:ET ratios during the Jun-Jul period in both years. The growing season average T:ET was approximately 0.82 in 2016 and 0.77 in 2017. Slightly smaller T:ET for the 2017 growing season can be attributed to more E at the expense of T due to more seasonal rainfall and greater availability of SM. Average near surface SM for the May-Oct period was approximately 0.10 and 0.15 m^3 m^{-3} in 2016 and 2017,

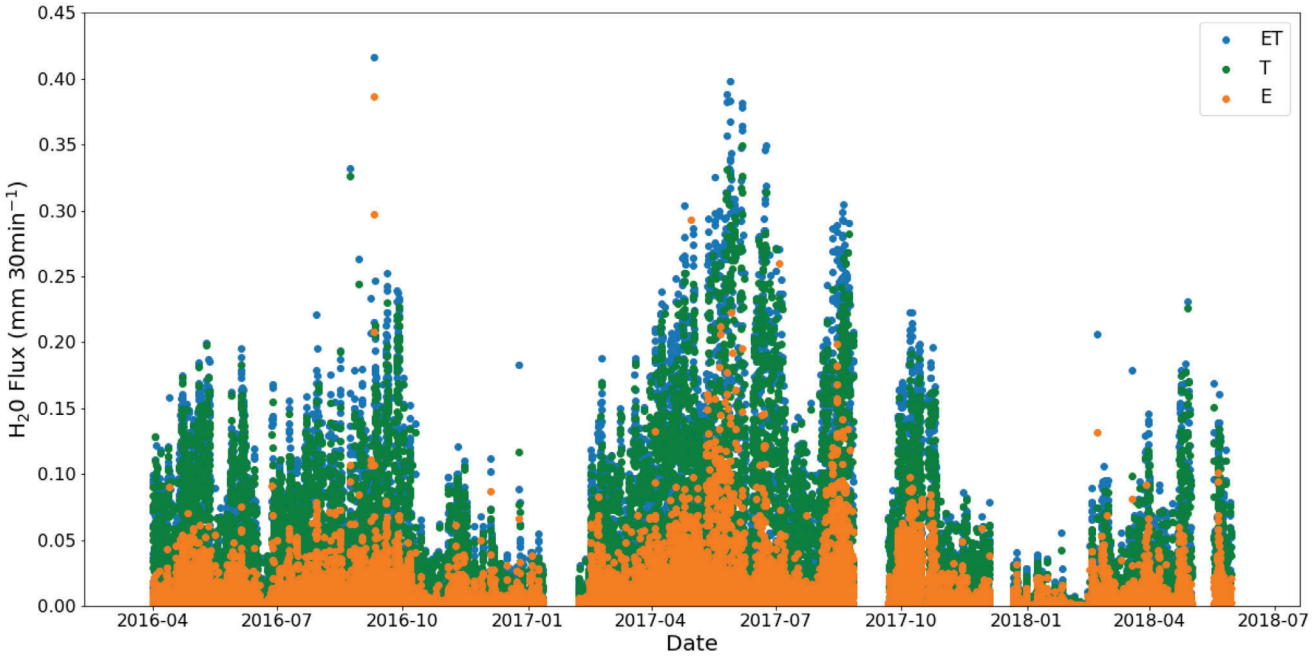

Fig. 2. Dynamics of evapotranspiration (ET) and partitioned fluxes (evaporation, E and transpiration, T) for the study period.

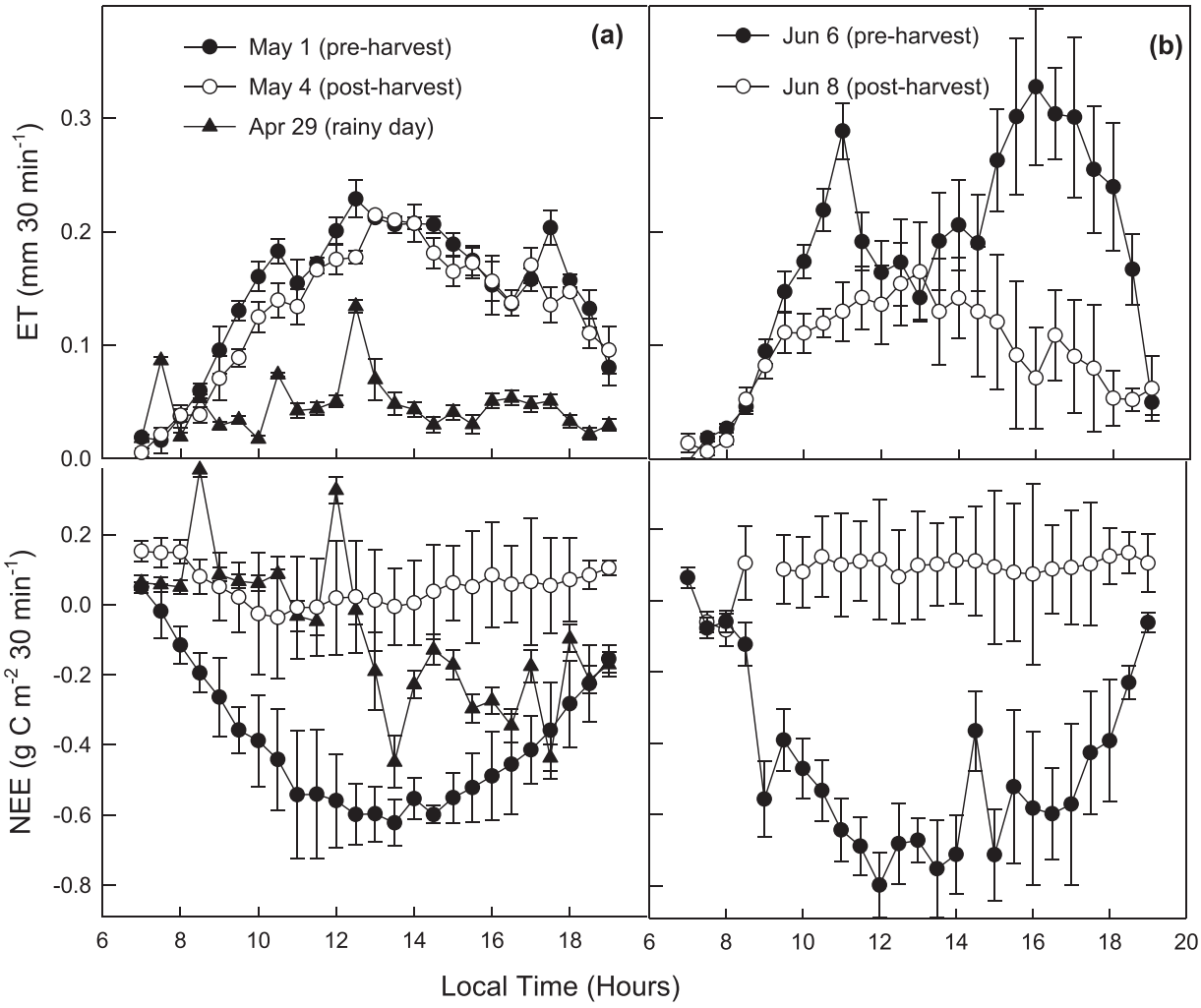

Fig. 3. Daytime (7:00 am - 7:00 pm local time) patterns of evapotranspiration (ET) and net ecosystem CO_2 exchange (NEE) for the selected days in 2017. The alfalfa field was harvested for hay on May 3 and Jun 7, 2017. Negative NEE indicates gain of carbon by the alfalfa field. Bars represent standard errors of the mean.

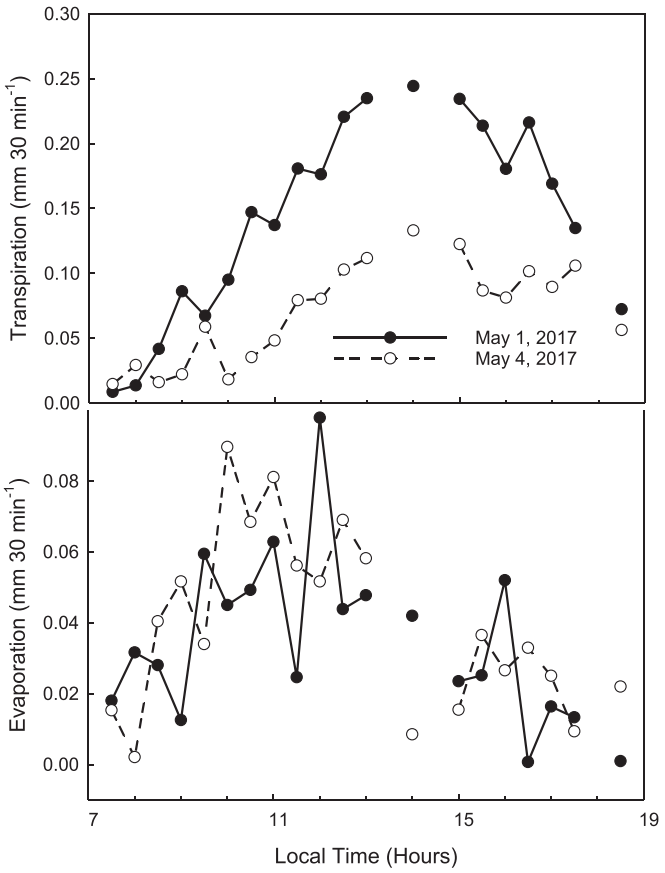

Fig. 4. Daytime (7:00 am - 7:00 pm local time) patterns of partitioned fluxes (transpiration and evaporation) for the selected pre-harvest (May 1) and post-harvest (May 4) days. The alfalfa field was harvested for hay on May 3.

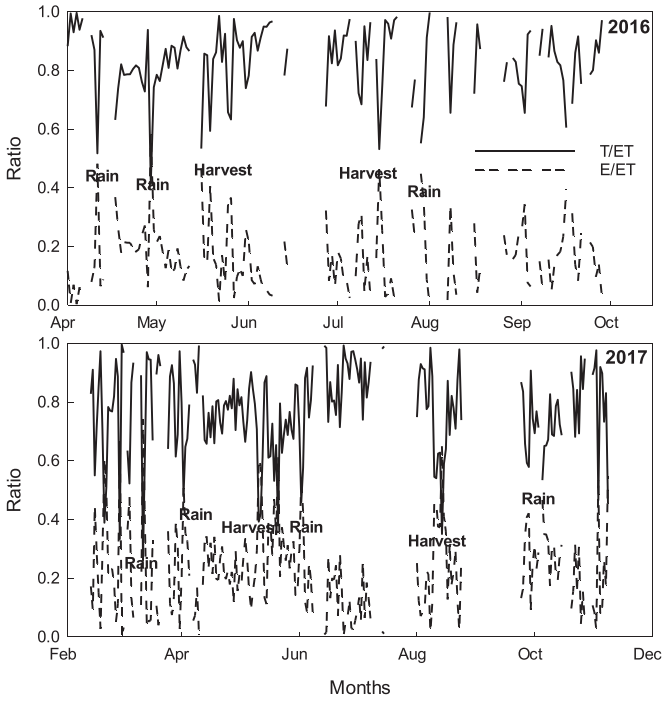

Fig. 5. Dynamics of the ratio of transpiration (T) or evaporation (E) to evapotranspiration (ET) during midday (averaged from 11:00 am to 2:00 pm local time) for the 2016 and 2017 alfalfa growing seasons. Few major rain and harvest events are marked.

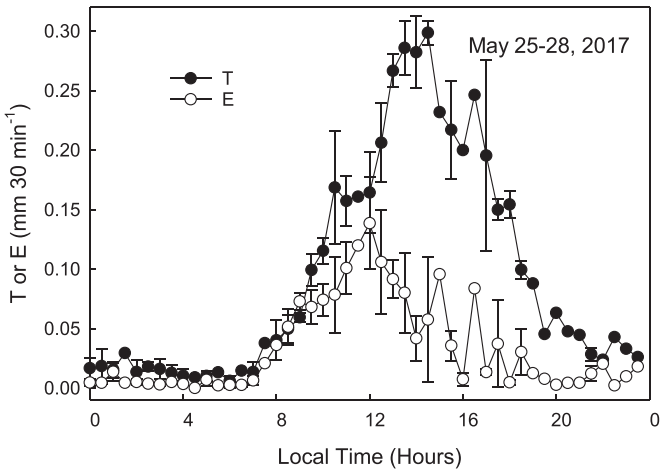

Fig. 6. Diurnal patterns of partitioned fluxes (evaporation, E and transpiration, T) for a selected period during a peak growth of alfalfa. Bars represent standard errors of the mean.

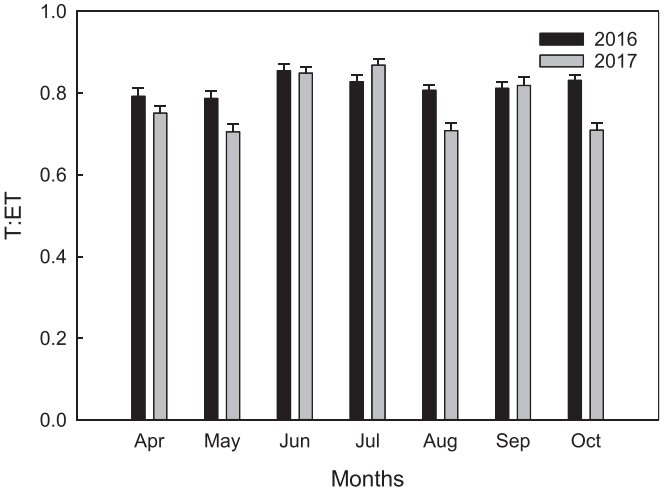

Fig. 7. Proportion of transpiration (T) to evapotranspiration (ET) for each month of the 2016 and 2017 growing seasons. Bars represent standard errors of the mean.

respectively. Transpiration of roughly 80% of seasonal ET in this study was on par with that reported for forests (Wang et al., 2014). They reported a range of 38–77% T of total ET based on synthesis of the available data from global-scale field measurements.

3.3. Diurnal variations of q-c correlation (R_{qc}) and leaf-level water use efficiency (WUE)

Mean diurnal cycles of R_{qc} and WUE were compared for the three selected periods: pre-harvest, post-harvest, and winter (Fig. 8a, b). Maximum anti-correlation (R_{qc} approaching −1) generally occurred at around local noon time when vegetation was the largest sink of c and the largest source of q. Decorrelation of q and c or dominance of non-photosynthetic fluxes of c and q (i.e., R and E) resulted in positive R_{qc} values during the evening, night, and early morning. As a result, R_{qc} showed a concave shape in diurnal cycle during all selected time periods. Peak values of R_{qc} were close to −1 (minimum of −0.94) for several hours (from 10:00 am to 4:00 pm local time) during May 1–15, 2016 (pre-harvest). In comparison, R_{qc} values reached a minimum of −0.55 and −0.58 at around noon during May 19–25, 2016 (post-harvest) and December 16–30, 2016 (winter), respectively. In addition, the diurnal correlation curve decayed quickly from midday. As a result,

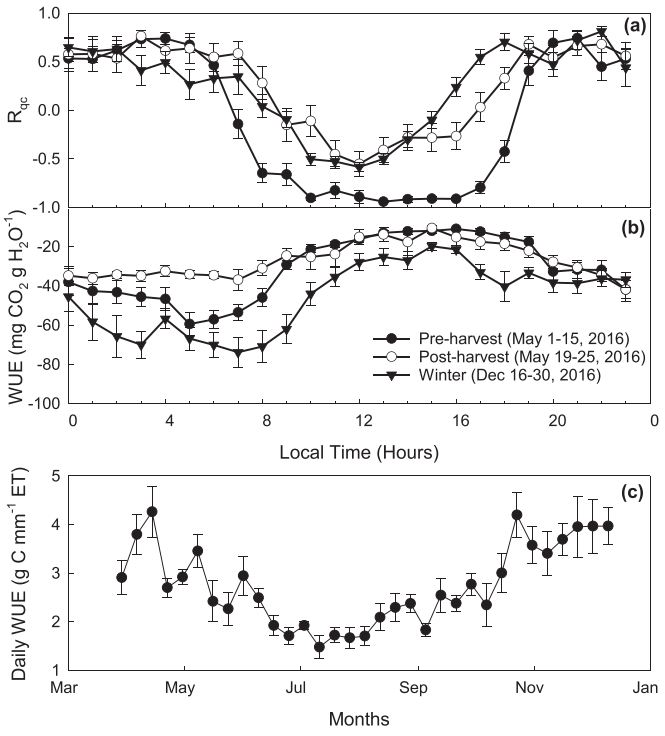

Fig. 8. Hourly binned diurnal courses of the correlation (R_{qc}) between carbon and water fluxes (a), and leaf-level water use efficiency (WUE, b) for the three selected periods, and seasonal dynamics of daily (weekly average) ecosystem WUE (c), computed as the ratio of sums of eddy covariance (EC)-derived gross primary production (GPP) to EC-measured evapotranspiration (ET) for the 2016 alfalfa growing season. Bars represent standard errors of the mean.

R_{qc} peaked only for a shorter period around noon during post-harvest and winter periods as compared to the pre-harvest period (Fig. 8a), illustrating that diurnal patterns of R_{qc} vary seasonally (Wang et al., 2016). Temporal changes in the dominant flux component (P vs. respiration (R) and T vs. E) due to changes in vegetation activity modulate R_{qc} and cause diurnal and seasonal trends of R_{qc}.

The diurnal pattern of R_{qc} followed the diurnal pattern of PPFD (Fig. 9a). The R_{qc} values were −0.5 or more negative when PPFD >400 μmol $m^{-2} s^{-1}$. The scatter plot also showed an abrupt transition in R_{qc} between 400–500 μmol $m^{-2} s^{-1}$, with R_{qc} transitioning towards −1 at higher PPFD (Fig. 9b). Wang et al. (2016) also reported a similar abrupt transition in R_{qc} for incoming solar radiation >200 W m^{-2} (equivalent to PPFD >400 μmol $m^{-2} s^{-1}$) at a suburban grass field in Princeton, New Jersey, USA. A strong linear relationship (R^2 = 0.78, Fig. 9c) between PPFD and T illustrated the dominance of T at higher PPFD. Dominant roles of T for q and P for c result in strong anti-correlations (R_{qc} close to −1) between q and c (Scanlon and Sahu, 2008; Williams et al., 2007). We did not find any trends for R_{qc}-T_a and R_{qc}-SM relationships, but R_{qc} quickly transitioned towards −1 with increasing VPD beyond 10 Pa (Fig. 9d). These results were consistent with the findings of Wang et al. (2016) that decorrelation between q and c at low VPD (humidity near saturation) can be caused by a sharp reduction in T but continuity of P.

Mean diurnal cycles of estimated WUE at the leaf-level by Eq. (1) followed similar patterns for the three selected periods: pre-harvest, post-harvest, and winter (Fig. 8b). During all periods, WUE was the highest (negative sign convention) in the early morning, decreased sharply with increasing solar radiation after sunrise, remained lower and stable level from noon to afternoon due to higher radiation and VPD, and increased again in the evening after radiation and VPD decreased. As a result, WUE showed negative relationships with radiation and VPD when multiple regression analysis was performed using half-hourly EC data (Wagle and Kakani, 2014a).

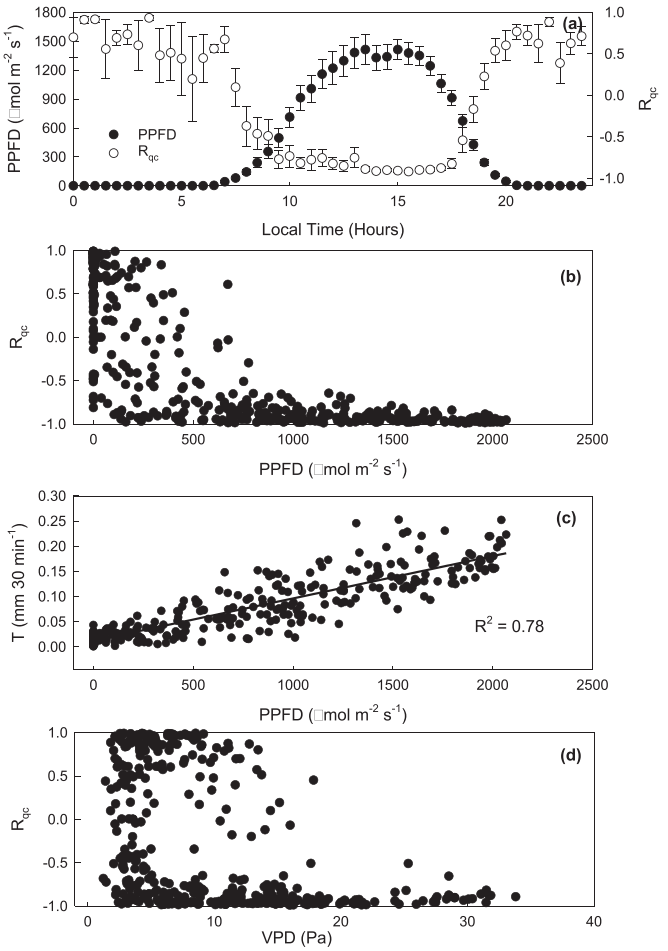

Fig. 9. Half-hourly binned diurnal courses (a) of the correlation between carbon and water fluxes (R_{qc}) and photosynthetic photon flux density (PPFD), and relationships of PPFD with R_{qc} (b) and transpiration (T, c), and relationship of vapor pressure deficit (VPD) with R_{qc} (d) for a selected period (Apr 15–28, 2017) during peak growth of alfalfa. Bars represent standard errors of the mean.

Large variability in diurnal cycles of leaf-level WUE for the three selected periods (Fig. 8b) indicated how the WUE pattern varied seasonally. Post-harvest period had the lowest and winter period had the highest WUE. Substantial amount of water can be lost as E but the carbon assimilation is low after harvesting of hay. Higher WUE in winter can be due to the fact that a perennial alfalfa stand can acquire substantial amounts of carbon in winter when ET demand is low. The magnitude of WUE was intermediate during peak growth due to a more rapid increase in water use than in carbon gain.

If direct measurements of WUE are not available, Fluxpart can estimate leaf-level WUE from atmospheric CO_2 and H_2O data, the photosynthetic pathway of the vegetation (C_3 or C_4), and the heights of the canopy and the EC system (Skaggs et al., 2018). Due to a lack of direct measurements, WUE was estimated in this manner for this study. The diurnal and temporal patterns of estimated WUE followed the expected trends as well as the seasonal dynamics of ecosystem level WUE (derived from EC-derived gross primary production (GPP) and EC-measured ET, Fig. 8c). The magnitudes of weekly ecosystem level WUE were >3.5 g C mm^{-1} ET during spring and winter but decreased to ~1.5 g C mm^{-1} ET or less during summer.

3.4. Seasonal variations of q-c correlation (R_{qc})

Daily average values of R_{qc} around midday (11:00 am – 2:00 pm

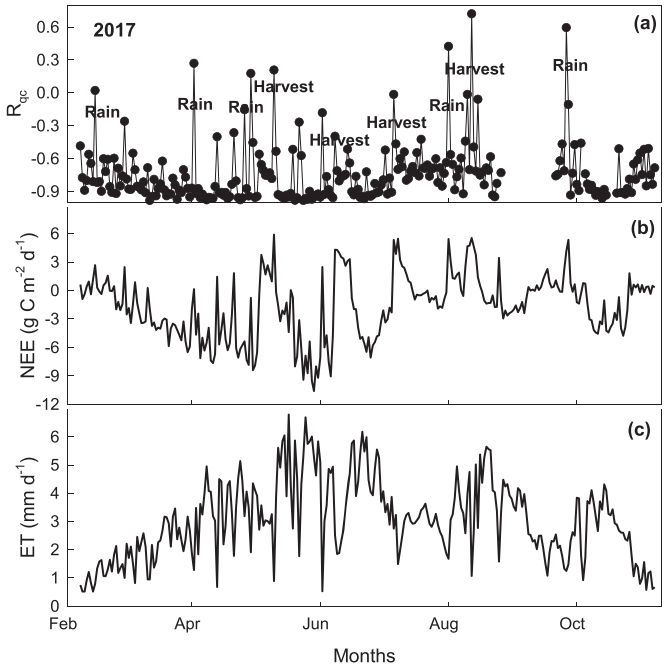

Fig. 10. Midday (11:00 am – 2:00 pm local time) average values of the correlation (R_{qc}) between carbon and water fluxes (a), and daily values of net ecosystem CO_2 exchange (NEE, b) and evapotranspiration (ET, c) for the 2017 alfalfa growing season. Few major rain and harvest events are marked.

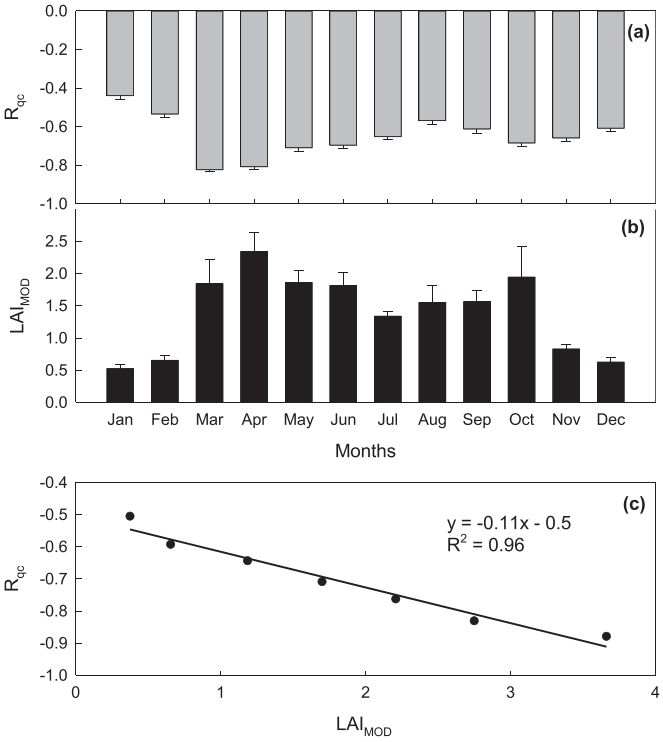

Fig. 11. Monthly midday (11:00 am – 2:00 pm local time) average values of the correlation (R_{qc}) between carbon and water fluxes (a), monthly average Moderate Resolution Imaging Spectroradiometer (MODIS)-derived leaf area index (LAI_{MOD}, b), and the relationship between them (LAI_{MOD} and R_{qc}, c). Data were binned for the entire study period. Bars represent standard errors of the mean.

local time), and daily NEE and ET during Feb-Nov 2017 are shown in Fig. 10. Daily NEE values were close to zero or positive and ET values were ~0.5 mm at the beginning and end of the growing season. Both NEE (negative is gain of carbon) and ET began to increase with growth of alfalfa vegetation. The R_{qc} transitioned towards −1 as the alfalfa field became a net sink of carbon. The R_{qc} values were close to −1 when NEE and ET peaked during peak growth. There was decorrelation or poor correlation between q and c during harvesting and rainy periods, due to an increase in fraction of direct E at the expense of the fractional contribution from T. Rain events and harvests had similar impacts on R_{qc}, NEE, and ET: ET decreased, NEE transitioned towards positive (source of carbon), and R_{qc} transitioned towards less negative or even positive. We did not observe a direct relationship of daily solar radiation, SM, or T_a with midday average R_{qc} (data not shown), similar to the findings of Wang et al. (2016).

3.5. Seasonality of R_{qc} with alfalfa vegetation growth

Monthly averaged midday (11:00 am – 2:00 pm local time) R_{qc} values and monthly averaged LAI_{MOD} for the study period are presented in Fig. 11 to show the seasonal variations of R_{qc} and alfalfa vegetation growth. The strongest q-c anti-correlation (R_{qc} towards −1) occurred during peak growth (Mar-Apr, as shown by the largest values of LAI_{MOD}) when T and P were dominant and co-regulated by the leaf stomata. The results also indicated that both q and c were jointly carried by turbulent structures. The field was not harvested for hay until May each year. Relatively smaller q-c anti-correlation and LAI_{MOD} values during summer can be attributed to monthly harvesting of hay from May to Jul each year as well as lower rainfall and drier top soils during the summer. Both q-c anti-correlation and LAI_{MOD} values were higher again in the fall due to more rainfall and no frequent harvest of hay. Due to close correspondence between vegetation growth and R_{qc}, a strong linear relationship (R^2 = 0.96) was observed between R_{qc} and LAI_{MOD} (Fig. 11c). The R_{qc} transitioned towards −1 as LAI_{MOD} of alfalfa increased. The result indicated that a one unit increase or decrease in LAI_{MOD} would increase or decrease R_{qc} by 0.11. Because of such changes in R_{qc} due to changes in vegetation cover, several studies have reported a strong control of vegetation on ET partitioning (Good et al., 2014; Schlesinger and Jasechko, 2014; Wang et al., 2010). A strong correspondence between R_{qc} and LAI_{MOD} in this study also indicated the potential of determining the seasonality of R_{qc} in alfalfa using remotely-sensed vegetative metrics.

4. Conclusions

The correlation between water vapor (q) and carbon dioxide (c) fluxes were examined with the FVS ET partitioning method using 10 Hz time series eddy covariance (EC) measurements over a non-irrigated alfalfa field. This ET partitioning method successfully reproduced the seasonal and inter-annual variations of partitioned E and T fluxes. Temporal variability of R_{qc} was consistent with the expected shifts in the dominance of T or E. The R_{qc} was strongly regulated by vegetation status, hay harvesting, and rainfall events. A strong linear relationship between R_{qc} and LAI_{MOD} offered the potential of determining the seasonality of R_{qc} in alfalfa using remotely-sensed vegetative metrics. Transpiration accounted for roughly 80% of the total ET during the alfalfa growing season. Since there are no additional equipment needed beyond a standard EC system for this partitioning method, it can be easily applied to existing EC datasets, which are available across locations and biomes, to better understand the trade-offs between carbon gain and water loss at the canopy scale. Ability of separating component fluxes, as demonstrated in this study, can be a useful tool not only to better interpret the measured fluxes but also to improve models of CO_2 and H_2O fluxes. This study can provide a foundation for future applications of this ET partitioning procedure at additional EC sites. However, further research is needed to determine the biases in partitioned fluxes using additional independent measurements of component fluxes.

Disclaimer

"Mention of trade names or commercial products in this publication is solely for the purpose of providing specific information and does not imply recommendation or endorsement by the U.S. Department of Agriculture."

"The U.S. Department of Agriculture (USDA) prohibits discrimination in all its programs and activities on the basis of race, color, national origin, age, disability, and where applicable, sex, marital status, familial status, parental status, religion, sexual orientation, genetic information, political beliefs, reprisal, or because all or part of an individual's income is derived from any public assistance program. (Not all prohibited bases apply to all programs.) Persons with disabilities who require alternative means for communication of program information (Braille, large print, audiotape, etc.) should contact USDA's TARGET Center at (202) 720-2600 (voice and TDD). To file a complaint of discrimination, write to USDA, Director, Office of Civil Rights, 1400 Independence Avenue, S.W., Washington, D.C. 20,250-9410, or call (800) 795-3272 (voice) or (202) 720-6382 (TDD). USDA is an equal opportunity provider and employer."

Declaration of Competing Interest

The authors declare that they have no known competing financial interests or personal relationships that could have appeared to influence the work reported in this paper.

Acknowledgments

This study was partly supported by a research grant (Project No. 2019-68012-29888) through the USDA-NIFA. We would like to thank a research technician, Shelby Robertson, for her assistance in screening the input files and running the Fluxpart partitioning codes.

References

Austin, A.T., et al., 2004. Water pulses and biogeochemical cycles in arid and semiarid ecosystems. Oecologia 141 (2), 221–235.
Baldocchi, D., 2014. Measuring fluxes of trace gases and energy between ecosystems and the atmosphere–the state and future of the eddy covariance method. Glob. Chang. Biol. 20 (12), 3600–3609.
Betts, A.K., Ball, J.H., Beljaars, A.C., Miller, M.J., Viterbo, P.A., 1996. The land surface-atmosphere interaction: a review based on observational and global modeling perspectives. J. Geophys. Res.. 101 (D3), 7209–7225.
Burt, C.M., Mutziger, A.J., Allen, R.G., Howell, T.A., 2005. Evaporation research: review and interpretation. J. Irrig. Drain. Eng. 131 (1), 37–58.
Cernusak, L.A., et al., 2018. Unsaturation of vapour pressure inside leaves of two conifer species. Sci. Rep. 8 (1), 7667.
Detto, M., Katul, G., 2007. Simplified expressions for adjusting higher-order turbulent statistics obtained from open path gas analyzers. Bound. Layer Meteorol. 122 (1), 205–216.
Ferretti, D., et al., 2003. Partitioning evapotranspiration fluxes from a Colorado grassland using stable isotopes: seasonal variations and ecosystem implications of elevated atmospheric CO_2. Plant Soil 254 (2), 291–303.
Good, S.P., et al., 2014. δ2H isotopic flux partitioning of evapotranspiration over a grass field following a water pulse and subsequent dry down. Water Resour. Res 50 (2), 1410–1432.
Herbst, M., Kappen, L., Thamm, F., Vanselow, R., 1996. Simultaneous measurements of transpiration, soil evaporation and total evaporation in a maize field in northern Germany. J. Exp. Bot. 47 (12), 1957–1962.
Katul, G.G., Palmroth, S., Oren, R., 2009. Leaf stomatal responses to vapour pressure deficit under current and CO2-enriched atmosphere explained by the economics of gas exchange. Plant Cell Environ. 32 (8), 968–979.
Kelliher, F., et al., 1992. Evaporation, xylem sap flow, and tree transpiration in a New Zealand broad-leaved forest. Agric. Meteorol. 62 (1–2), 53–73.
Klosterhalfen, A., et al., 2019a. Source partitioning of H 2 O and CO 2 fluxes based on high-frequency eddy covariance data: a comparison between study sites. Biogeosciences 16 (6), 1111–1132.
Klosterhalfen, A., et al., 2019b. Sensitivity analysis of a source partitioning method for H2O and CO2 fluxes based on high frequency eddy covariance data: findings from field data and large eddy simulations. Agric. Meteorol. 265, 152–170.
Kool, D., et al., 2014. A review of approaches for evapotranspiration partitioning. Agric. Meteorol. 184, 56–70.
Law, B., et al., 2002. Environmental controls over carbon dioxide and water vapor exchange of terrestrial vegetation. Agric. Meteorol. 113 (1), 97–120.
Lawrence, D.M., Thornton, P.E., Oleson, K.W., Bonan, G.B., 2007. The partitioning of evapotranspiration into transpiration, soil evaporation, and canopy evaporation in a GCM: impacts on land–atmosphere interaction. J. Hydrometeorol. 8 (4), 862–880.
Massman, W., 1998. A review of the molecular diffusivities of H2O, CO2, CH4, CO, O3, SO2, NH3, N2O, NO, and NO2 in air, O2 and N2 near STP. Atmos. Environ. 32 (6), 1111–1127.
Matheny, A.M., et al., 2014. Species-specific transpiration responses to intermediate disturbance in a northern hardwood forest. J. Geophys. Res. 119 (12), 2292–2311.
Miralles, D., De Jeu, R., Gash, J., Holmes, T., Dolman, A., 2011. Magnitude and variability of land evaporation and its components at the global scale. Hydrol. Earth Sys. Sci. 15, 967–981.
Morales, P., et al., 2005. Comparing and evaluating process-based ecosystem model predictions of carbon and water fluxes in major European forest biomes. Glob. Chang. Biol. 11 (12), 2211–2233.
Morison, J.I., Gifford, R.M., 1983. Stomatal sensitivity to carbon dioxide and humidity a comparison of two C3 and two C4 grass species. Plant Physiol. 71 (4), 789–796.
Norman, J.M., Kustas, W.P., Humes, K.S., 1995. Source approach for estimating soil and vegetation energy fluxes in observations of directional radiometric surface temperature. Agric. Meteorol. 77 (3), 263–293.
ORNL D.A.A.C., 2017. MODIS collection 6 land products global subsetting and visualization tool. ORNL DAAC, Oak Ridge, Tennessee, USA. 10.3334/ORNLDAAC/1379.
Palatella, L., Rana, G., Vitale, D., 2014. Towards a flux-partitioning procedure based on the direct use of high-frequency eddy-covariance data. Bound. Layer Meteorol. 153 (2), 327–337.
Peddinti, S.R., Kambhammettu, B.P., 2019. Dynamics of crop coefficients for citrus orchards of central India using water balance and eddy covariance flux partition techniques. Agric. Water Manag. 212, 68–77.
Perez-Priego, O., et al., 2018. Partitioning eddy covariance water flux components using physiological and micrometeorological approaches. J. Geophys. Res. 123 (10), 3353–3370.
Rana, G., Palatella, L., Scanlon, T.M., Martinelli, N., Ferrara, R.M., 2018. CO2 and H2O flux partitioning in a Mediterranean cropping system. Agric. Meteorol. 260, 118–130.
Scanlon, T.M., Kustas, W.P., 2010. Partitioning carbon dioxide and water vapor fluxes using correlation analysis. Agric. Meteorol. 150 (1), 89–99.
Scanlon, T.M., Kustas, W.P., 2012. Partitioning evapotranspiration using an eddy covariance-based technique: improved assessment of soil moisture and land–atmosphere exchange dynamics. Vadose Zone J. 11 (3).
Scanlon, T.M., Sahu, P., 2008. On the correlation structure of water vapor and carbon dioxide in the atmospheric surface layer: a basis for flux partitioning. Water Resour. Res. 44 (10).
Scanlon, T.M., Schmidt, D.F., Skaggs, T.H., 2019. Correlation-based flux partitioning of water vapor and carbon dioxide fluxes: method simplification and estimation of canopy water use efficiency. Agric.Meteorol. 279, 107732.
Schlesinger, W.H., Jasechko, S., 2014. Transpiration in the global water cycle. Agric. Meteorol. 189, 115–117.
Simunek, J., Van Genuchten, M.T., Sejna, M., 2005. The HYDRUS-1D software package for simulating the one-dimensional movement of water, heat, and multiple solutes in variably-saturated media. Uni. California-Riverside Res. Rep. 3, 1–240.
Skaggs, T., Anderson, R., Alfieri, J., Scanlon, T., Kustas, W., 2018. Fluxpart: open source software for partitioning carbon dioxide and water vapor fluxes. Agric. Meteorol. 253, 218–224.
Sperry, J.S., Love, D.M., 2015. What plant hydraulics can tell us about responses to climate-change droughts. New Phytologist. 207 (1), 14–27.
Sulman, B.N., Roman, D.T., Scanlon, T.M., Wang, L., Novick, K.A., 2016. Comparing methods for partitioning a decade of carbon dioxide and water vapor fluxes in a temperate forest. Agric. Meteorol. 226, 229–245.
Sutanto, S., Wenninger, J., Coenders-Gerrits, A., Uhlenbrook, S., 2012. Partitioning of evaporation into transpiration, soil evaporation and interception: a comparison between isotope measurements and a HYDRUS-1D model. Hydrol. Earth Syst. Sci. 16 (8), 2605–2616.
Sutanto, S.J., et al., 2014. HESS opinions: a perspective on isotope versus non-isotope approaches to determine the contribution of transpiration to total evaporation. Hydrol. Earth Syst. Sc. 18 (8), 2815–2827.
Wagle, P., Gowda, P.H., Northup, B.K., 2019a. Annual dynamics of carbon dioxide fluxes over a rainfed alfalfa field in the US Southern Great Plains. Agric. Meteorol. 265, 208–217.
Wagle, P., Gowda, P.H., Northup, B.K., 2019b. Dynamics of evapotranspiration over a non-irrigated alfalfa field in the Southern Great Plains of the United States. Agric. Water Manag. 223, 105727.
Wagle, P., Kakani, V.G., 2014a. Growing season variability in evapotranspiration, ecosystem water use efficiency, and energy partitioning in switchgrass. Ecohydrology 7 (1), 64–72.
Wagle, P., Kakani, V.G., 2014b. Seasonal variability in net ecosystem carbon dioxide exchange over a young Switchgrass stand. GCB Bioenergy 6 (4), 339–350.
Wang, L., et al., 2010. Partitioning evapotranspiration across gradients of woody plant cover: assessment of a stable isotope technique. Geophys. Res. Lett. 37 (9).
Wang, L., Good, S.P., Caylor, K.K., 2014. Global synthesis of vegetation control on evapotranspiration partitioning. Geophys. Res. Lett. 41 (19), 6753–6757.
Wang, P., Yamanaka, T., Li, X.-Y., Wei, Z., 2015. Partitioning evapotranspiration in a temperate grassland ecosystem: numerical modeling with isotopic tracers. Agric. Meteorol. 208, 16–31.
Wang, W., et al., 2016. On the correlation of water vapor and CO2: application to flux partitioning of evapotranspiration. Water Resour. Res. 52 (12), 9452–9469.
Webb, E.K., Pearman, G.I., Leuning, R., 1980. Correction of flux measurements for density effects due to heat and water vapour transfer. Q. J. Royal Meteorol. Soc. 106 (447), 85–100.

Wilcox, B., Seyfried, M., Breshears, D., Stewart, B., Howell, T., 2003. The water balance on rangelands. Encycl. of Water Sci. 791–794.
Williams, C.A., Scanlon, T.M., Albertson, J.D., 2007. Influence of surface heterogeneity on scalar dissimilarity in the roughness sublayer. Bound. Layer Meteorol. 122 (1), 149.
Williams, D., et al., 2004. Evapotranspiration components determined by stable isotope, sap flow and eddy covariance techniques. Agric. Meteorol. 125 (3–4), 241–258.
Wutzler, T., et al., 2018. Basic and extensible post-processing of eddy covariance flux data with REddyProc. Biogeosciences 15 (16), 5015–5030.
Yepez, E.A., et al., 2005. Dynamics of transpiration and evaporation following a moisture pulse in semiarid grassland: a chamber-based isotope method for partitioning flux components. Agric. Meteorol. 132 (3), 359–376.